Nic96p Is Required for Nuclear Pore Formation and Functionally Interacts with a Novel Nucleoporin, Nup188p

Ulrike Zabel,* Valérie Doye,‡ Hildegard Tekotte,§ Roger Wepf,§ Paola Grandi,‖ and Eduard C. Hurt‖

*University of Würzburg, Institut für Pharmakologie und Toxikologie, D-97078 Würzburg, Germany;‡Centre National de la Recherche Scientifique, UMR144, Institut Curie, Section du Recherche, 75231 Paris Cedex 5, France;§European Molecular Biology Laboratory, D-69117 Heidelberg, Germany; and‖University of Heidelberg, Biochemie I, D-69120 Heidelberg, Germany

Abstract. The amino-terminal domain of Nic96p physically interacts with the Nsp1p complex which is involved in nucleocytoplasmic transport. Here we show that thermosensitive mutations mapping in the central domain of Nic96p inhibit nuclear pore formation at the nonpermissive temperature. Furthermore, the carboxy-terminal domain of Nic96p functionally interacts with a novel nucleoporin Nup188p in an allele-specific fashion, and when ProtA-Nup188p was affinity purified, a fraction of Nic96p was found in physical interaction. Although *NUP188* is not essential for viability, a null mutant exhibits striking abnormalities in nuclear envelope and nuclear pore morphology. We propose that Nic96p is a multivalent protein of the nuclear pore complex linked to several nuclear pore proteins via its different domains.

NUCLEAR pore complexes (NPCs)[1] form proteinaceous channels across the nuclear envelope, allowing both active and passive transport of a broad variety of substrates between the nucleus and cytoplasm. The 120-MD structure of the NPC in higher eukaryotes shows an elaborate fine structure in the EM (for review, see Panté and Aebi, 1994) and this basic architecture seems to be also shared by the smaller 66-MD yeast NPC, indicating a high degree of evolutionary conservation (Rout and Blobel, 1993). NPCs are capable of accommodating different transport substrates such as proteins and RNPs in a bidirectional fashion (for reviews see Powers and Forbes, 1994; Simos and Hurt, 1995) and it is clear that the different transport processes through the NPC require soluble factors for the substrate recognition and translocation. Recently, the receptor for the nuclear localization sequence (NLS), which targets nuclear proteins to the nuclear periphery, was identified (Adam and Adam, 1994; Görlich et al., 1994; Enenkel et al., 1995; Moroianu et al., 1995; Radu et al., 1995; Weis et al., 1995). The translocation step through the pore channnel is dependent on further soluble factors, the small GTP-binding protein Ran/TC4 (Moore and Blobel, 1993; Melchior et al., 1993; Schlenstedt et al., 1995), and pp15/NTF2 (Moore and Blobel, 1994; Paschal and Gerace, 1995). Similarly, export of RNA requires soluble nuclear factors; for example, snRNA export depends on a nuclear cap-binding protein complex (Izaurralde et al., 1994).

Over the past years, several of the maybe 50–100 different NPC proteins (nucleoporins) were identified and cloned from different organisms using biochemical, immunological, and genetic strategies (for reviews see Rout and Wente, 1994; Doye and Hurt, 1995). Some of them could be localized to distinct substructures of the NPC; among these, gp210, Pom121p, and Pom152p, which are integral membrane proteins of the pore membrane, were suggested to play a role in anchoring the NPC within the nuclear membrane (Greber et al., 1990; Hallberg et al., 1993; Wozniak et al., 1994); other nucleoporins such as p62 were shown to be components of the central pore channel complex (Grote et al., 1995), the cytoplasmic fibrils (NUP180, NUP214), and the nuclear basket (NUP153) (Wilken et al., 1993; Panté et al., 1994).

Many nucleoporins, both from yeast and vertebrates, share characteristic repeat sequences of the GLFG and/or XFXFG type. Recently, the GLFG repeats from Nup98p were shown to bind the complex formed between a karyophilic protein and the NLS receptor (Radu et al., 1995). Other motifs found in nucleoporins, which are suggestive of certain protein functions, are sequences involved in DNA binding (Sukegawa and Blobel, 1993; Yokoyama et al., 1995), RNA-binding (Fabre et al., 1994), binding of the small GTPase Ran/TC4 (Görlich and Hartmann, 1995; Yokoyama et al., 1995), and formation of coiled-coil structures (Hurt, 1990; Grandi et al., 1993; Buss et al., 1994).

Mutational analysis of nucleoporins in yeast revealed roles in different NPC functions. Temperature-sensitive mutants of Nsp1p (Nehrbass et al., 1993), Nup49p (Doye et al., 1994), Nup1p (Bogerd et al., 1994), and Nic96p (Grandi et

Address all correspondence to Dr. Eduard C. Hurt, University of Heidelberg, Biochemie I, Im Neuenheimer Feld 328, D-69120 Heidelberg, Germany. Tel.: 49 6221 54 41 73. Fax: 49 6221 54 43 69. E-mail: IN% cg5@ix.urz.uni-heidelberg.de''

1. *Abbreviations used in this paper:* NPC, nuclear pore complex; sl, synthetic lethal.

al., 1995*b*) were impaired in uptake of a nuclear reporter protein, suggesting a role in nuclear protein import; mutants of Nup116p (Wente and Blobel, 1993), Nup145p (Fabre et al., 1994), Nup49p (Doye et al., 1994), Nup1p (Bogerd et al., 1994; Schlaich and Hurt, 1995), Rat3p/Nup133p (Doye et al., 1994; Li et al., 1995), Nup82p (Grandi et al., 1995*a*), and Nup159p (Gorsch et al., 1995) are defective in poly(A)$^+$ RNA export. However, mutations in NPC proteins not only impair transport reactions, but often affect concomitantly nuclear envelope and NPC organization (Wente and Blobel, 1993, 1994; Doye et al., 1994; Gorsch et al., 1995; Pemberton et al., 1995).

To study NPC formation and how newly synthesized nuclear pore complexes become inserted into the nuclear envelope, *Xenopus* egg and HeLa extracts were used to reconstitute nuclei in vitro, comprising an intact nuclear membrane with numerous NPCs (Burke and Gerace, 1986; Newport, 1987; Dabauvalle and Scheer, 1991). The in vitro assembly of transport-competent NPCs was shown to depend on nucleoporin p62, but whether p62 is also required for NPC formation is still not clear (Dabauvalle et al., 1990; Finlay and Forbes, 1990; Finlay et al., 1991). Similarly, transcriptional repression of Nsp1p expression from yeast cells leads to an impaired nuclear transport as well as a decrease in NPC density (Mutvei et al., 1992). On the other hand, depletion of nucleoporin p97, from *Xenopus* egg extracts, leads to formation of transport-competent nuclei, which are defective in nuclear growth and replication of chromosomal DNA (Powers et al., 1995).

To understand how nucleoporins are involved in NPC formation and nucleocytoplasmic transport, it is also important to find out how they interact with each other both physically and functionally. So far only a few of these relationships, and subcomplexes of nucleoporins have been defined (Dabauvalle et al., 1990; Finlay et al., 1991; Kita et al., 1993; Panté et al., 1994; Buss and Stewart, 1995; Grandi et al., 1995*a*,*b*; Macaulay et al., 1995).

In this paper we further investigated the functional roles of the different Nic96p domains. The amino-terminal coiled-coil domain of Nic96p was already shown to interact with the Nsp1p/Nup57p/Nup49p core complex (Grandi et al., 1995*b*). We now show that mutations mapping in the central domain of Nic96p affect NPC biogenesis. To obtain insight into the function of the nonessential COOH-terminal domain of Nic96p, we screened for mutants that caused synthetic lethality when this part of Nic96p was missing. In that way, we identified a novel nucleoporin Nup188p which on its own has also a role in nuclear pore biogenesis.

Materials and Methods

Yeast Strains and Plasmids

The yeast strains used in this study are listed in Table I. Microbiological techniques were performed essentially as described in Grandi et al. (1995*b*) and Wimmer et al. (1992). The following plasmids were used in this study: pUN100, *ARS/CEN* plasmid with the *LEU2* marker (Elledge and Davis, 1988); pRS314, *ARS/CEN* plasmid with the *TRP1* marker (Sikorski and Hieter, 1989); pUN100-NIC96 (Grandi et al., 1993); pUN100-nic96-1 (P332L; L260P) (Grandi et al., 1995*b*); pUN100-nic96-2 (W334R) (Grandi et al., 1995*b*); pUN100-nic96Δ28-63 (Grandi et al., 1995*b*); pRS314-nic96-1, a *Sph*I blunt-ended/*Sac*I fragment was excised from pUN100-nic96-1 and inserted into pRS314 cut with *Sma*I/*Sac*I; pSB32-NSP1, ARS1/CEN4 plasmid with the *LEU2* marker encoding the NSP1 carboxy-terminal domain under the control of the ADH1 promoter (Nehrbass et al., 1990).

For pUN100-ProtA-NIC96, the DNA encoding two synthetic IgG-binding domains from protein A under control of the *NOP1* promoter (Wimmer et al., 1992), fused in-frame to the ATG start codon of *NIC96* (described in Grandi et al., 1993), was cloned into pUN100. pUN100-ProtA-nic96-1 was constructed in a similar way. For construction of pUN100-nic96Δ525-839, a *Bam*HI site was created at nucleotide position 2100 in the pUN100-NIC96 (Grandi et al., 1993) by PCR. The *Bam*HI site was opened, filled in by Klenow, and an oligoterminator (Grandi et al., 1995*a*) was inserted. The resulting nucleotide sequence around the fusion site is CGC TTG GAT CTA ACT GAG TAG. The deduced amino acid sequence is R(523)-L(524)-D-L-T-E stop codon, with the last four amino

Table I. Yeast Strains

Strain	Genotype
RS453	**a**/α, *ade2/ade2, tryp1/trp1, leu2/, ura3/ura3, his3/his3*
NIC96 shuffle	**a**, *ade2, trp1, leu2, ura3, HIS3::nic96* (pCH1122-URA3-ADE3-NIC96) (Grandi et al., 1995*a*; RS453-derivative)
Nic96	**a**, α*de2, trp1, leu2, ura3, HIS3::nic96* (pUN100-LEU2-NIC96)
nic96-1	**a**, α*de2, trp1, leu2, ura3, HIS3::nic96* (pUN100-LEU2-nic96^{ts} [P332L;L260P])
nic96-2	**a**, α*de2, trp1, leu2, ura3, HIS3::nic96* (pUN100-LEU2-nic96^{ts} [W334R])
nic96Δ28-63	**a**, α*de2, trp1, leu2, ura3, HIS3::nic96* (pUN100-LEU2-nic96^{ts} [Δ28-63])
ProtA-Nic96	**a**, α*de2, trp1, leu2, ura3, HIS3::nic96* (pUN100-LEU2-ProtA-NIC96)
ProtA-nic96-1	**a**, *ade2, trp1, leu2, ura3, his3::nic96* (pUN100-LEU2-ProtA-nic96-1)
CH1462	α, *ade2, ade3, trp1, leu2, ura3, his3*
CH/nic96	**a**/α, *ade2/ade2, ade3/ADE3, trp1/trp1, leu2/leu2, ura3/ura3, his3/HIS3::nic96* derived from crossing CH1462 × NIC96 shuffle
Red/white shuffle	*ade2, ade3, trp1, leu2, ura3, HIS3::nic96* (pCH1122-URA3-ADE3-NIC96) haploid progeny derived from CH/nic96
Screening strain	*ade2, ade3, trp1, leu2, ura3, HIS3::nic96* (pCH1122-URA3-ADE3-NIC96; pUN100-LEU2-nic96[Δ525-839])
s17	*ade2, ade3, trp1, leu2, ura3, HIS3::nic96, nup188-7* (pCH1122-URA3-ADE3-NIC96) (pUN100-LEU2-nic96[Δ525-839])
s122	*ade2, ade3, trp1, leu2, ura3, HIS3::nic96, nup188-22* (pCH1122-URA3-ADE3-NIC96)(pUN100LEU2-nic96[Δ525-839])
s123	*ade2, ade3, trp1, leu2, ura3, HIS3::nic96, nup188-23* (pCH1122-URA3-ADE3-NIC96)(pUN100LEU2-nic96[Δ525-839])
nup188$^-$	α, *ade2, ade3, trp1, leu2, ura3, HIS3::nup188* (derived from RS453)
Myc-Nup188	α, *ade2, trp1, leu2, ura3, HIS3::nup188* (pUN100-LEU2-Myc-Nup188)

acids coming from the terminator sequence. For pRS314-nic96Δ525-839, a *Sph*I blunt-ended/*Sac*I fragment was excised from pUN100-nic96Δ525-839 and inserted into pRS314 cut open at *Sma*I/*Sac*I.

Affinity Purification of ProtA Fusion Proteins

For affinity purification of the fusion proteins, ProtA-Nic96p, ProtA-nic96-1p, and ProtA-Nup188p strains were grown in 500 ml yeast extract peptone dextrose (YPD) medium at 23°C, harvested at OD_{600} 1.0–1.5, converted into spheroplasts, and lysed in 30–50 ml (10 ml/g cells) lysis buffer (2% Triton X-100, 150 mM NaCl, 5 mM $MgCl_2$, 20 mM Tris-HCl, pH 8.0, protease inhibitor cocktail) with a Dounce homogenizer. The homogenate was centrifuged for 10 min at 15,000 rpm in a Sorvall SS34 rotor. The supernatant was loaded on a 200-μl IgG-Sepharose column (Pharmacia, Freiburg, Germany) essentially as described earlier for ProtA-NSP1 purification (Grandi et al., 1993). Aliquots were analyzed by SDS-PAGE and silver staining or Western blotting; blots were decorated with the following antibodies: rabbit IgG coupled to HRP (protein A detection; DAKO-PATTS, Copenhagen, Denmark), anti-FSFG rabbit polyclonal serum (Nehrbass et al., 1990), anti-Nup49p polyclonal serum (Hurt, E.C., unpublished data), anti-Nup57p and anti-Nic96p peptide antisera (Grandi et al., 1995*b*). As a second antibody, goat anti–rabbit IgG coupled to alkaline phosphatase or HRP (Bio-Rad Laboratories, Hercules, CA) was used.

Analysis of Association of Nic96p with ProtA-Nup188p

To test for a physical association between Nic96p and Nup188p, the ProtA-Nup188p fusion protein was first bound to IgG-Sepharose beads, extensively washed with a 200-fold bead vol of TST buffer (0.05% Tween 20, 150 mM NaCl, 50 mM Tris, pH 8.0) before the $MgCl_2$-induced elution was performed. The last 2 ml of the wash fraction, as well as 2 ml $MgCl_2$-induced eluate fractions (steps from 0.6 to 4.5 M $MgCl_2$ in 0.05% Triton X-100, 50 mM Tris-HCl, pH 7.4 according to Siniossoglou et al., 1996) were collected, dialyzed 2 h against 50 mM Tris-HCl, pH 7.4, at 4°C, and concentrated 20-fold by ultrafiltration to 100 μl. These fractions were analyzed by SDS-PAGE and Western blotting, using anti-Nic96p (Grandi et al., 1995*b*), anti-Nup85p (Siniossoglou et al., 1996), and anti-Pus1p antibodies (Simos et al., 1996) in a 1:500 dilution, followed by rabbit IgG coupled to HRP in a 1:1,000 dilution. Note that a fourfold equivalent of the last wash fraction (see Fig. 4 *C*, lane *3*) as compared with the corresponding $MgCl_2$-derived eluate fractions (see Fig. 4 *C*, lanes *4–6*) was loaded on the gel.

The anti-Nic96p, anti-Nup85p, and anti-Pus1p antibodies used in the Western blots of Fig. 4, *B* and *C* were affinity purified rabbit polyclonal peptide antibodies. These antibodies not only specifically react via their variable region with their corresponding antigens, but also with the protein A moiety of the ProtA-Nup188p fusion protein and its many breakdown products which still have the ProtA tag on. The latter cross-reactivity is due to the fact that any rabbit IgG will react via its F_c part with protein A. Thus, affinity purified anti-Nic96p, anti-Nup85p, and anti-Pus1p IgG antibodies will automatically react with the ProtA-Nup188p fusion protein and its breakdown products.

Isolation of Synthetic Lethal (sl) Mutants of nic96Δ525-839

To obtain a *HIS::nic96* strain with the *ade2/ade3* markers required for the red/white colony sectoring assay (Wimmer et al., 1992), the NIC96 shuffle strain was crossed to the CH1462 strain (see Table I). The diploid CH/nic96 strain was sporulated, and a haploid progeny *HIS::nic96, ade2, ade3* plus pCH1122-URA3-ADE3-NIC96 was isolated after tetrad analysis. The sl screen was performed with the nic96Δ525-839 allele. To do so, the red/white shuffle strain was transformed with pUN100-LEU2-nic96Δ525-839. The resulting screening strain formed red/white sectoring colonies on SDC-leu plates containing 1.7 mg/ml adenine (Wimmer et al., 1992). UV mutagenesis was carried out essentially as described previously (Wimmer et al., 1992; Grandi et al., 1995*b*), and 30,000 surviving colonies were screened for a red, nonsectoring phenotype at 30°C. 7 colonies finally showed a stable nonsectoring phenotype after two rounds of restreaking and could not grow on 5-FOA plates. To analyze them further, cells were allowed to lose the pUN100-LEU2-nic96Δ525-839 plasmid, and leu$^-$ cells were transformed with pRS314-TRP1-nic96Δ525-839. Subsequently, cells were transformed with pUN100-NIC96 or pUN100-nic96Δ525-839. Only sl7, sl22, and sl23 were complemented by *NIC96* (i.e., they displayed a red/white sectoring phenotype and could grow on 5-FOA–containing plates), but not by *nic96Δ525-839*. sl7, sl22, and sl23 were then transformed by different LEU2 plasmids containing the genes of different cloned nucleoporins; all sl strains were found to be complemented by *NUP188*, but not by the other nucleoporin genes. To analyze allele specificity of the synthetically lethal interaction between *NUP188* and *NIC96*, the sl7, sl22, and sl23 strains, which had lost the pUN100-LEU2-nic96Δ525-839 plasmid (see above), were transformed with pUN100-LEU2 plasmids containing the *NIC96*, *nic96-1*, *nic96-2*, *nic96Δ28-63*, and *nic96Δ525-839* alleles, respectively, and tested for growth on 5-FOA–containing plates.

Cloning, Sequencing, and Disruption of NUP188

In a previous sl screen starting with a thermosensitive *nsp1* allele, a collection of red, nonsectoring sl strains was obtained (Grandi et al., 1995*b*). One of these sl strains, sl400, was transformed with a genomic library generated in pUN100 (described in Wimmer et al., 1992), and cells displaying a red/white sectoring phenotype and growth on 5-FOA–containing plates were obtained. A complementing plasmid, designated pUN100-NUP188, was recovered, and subfragments covering the entire complementing activity were cloned into pBluescript or pUN100 for DNA sequence analysis of both strands according to Sanger et al. (1977).

For disruption of the *NUP188* gene, a 3-kb *Xba*I/*Xho*I fragment was subcloned into pBluescript. A 2.5-kb *Sma*I/*Sal*I fragment (amino acids 399–1225) was excised, thereby removing 826 of the 1,655 amino acids of the *NUP188* open reading frame, and replaced by a 1.1-kb *Sma*I/*Sal*I fragment containing the *HIS3* gene from plasmid YDp-H. The *Xba*I/*Xho*I fragment containing the *nup188::HIS3* fragment was excised and used to transform the diploid RS453 strain. HIS$^+$ transformants were characterized for correct integration of the *nup188::HIS3* fragment at the *NUP188* locus by Southern blot analysis. Diploids heterozygous for *NUP188* were sporulated, and nup188$^-$ haploid progeny was identified by tetrad analysis.

Construction of myc- and Protein A–tagged Nup188p

A DNA fragment containing three myc epitopes in tandem (Siniossoglou et al., 1996) was cloned under the control of the *NOP1* promoter in pUN100. A *Spe*I/*Pst*I fragment comprising the *NOP1* promoter (pNOP1) and the triple myc epitope was excised. A 2.4-kb fragment of *NUP188*, coding for the first 810 amino acids, was amplified by PCR, using an internal 3′ primer and the 5′ primer TTT CTG CAG GCT ACA CCT TCA TTT GGC, thereby creating a *Pst*I site just after the ATG start codon of *NUP188*. A *Pst*I/*Nco*I fragment was then ligated in frame with the pNOP1/Myc fragment into pUN100-Nup188 opened at *Spe*I/*Nco*I, resulting in pUN100-Myc-Nup188. To obtain the ProtA-Nup188p, a 0.8-kb *Nhe*I/*Xba*I PCR fragment coding for four IgG-binding domains of ProtA (Grandi et al., 1995) was inserted in frame into the *Xba*I site of *NUP188*, located 324 bp (104 amino acids) downstream of the ATG start codon. The *HIS3* gene was cloned into the *Snab*I site within the 5′ noncoding region of *NUP188*. A 4-kb DNA fragment consisting of 5′ noncoding sequences of *NUP188* followed by the *HIS3* and *NUP188* gene tagged with *PROTA* sequences at the *Xba*I site, was used for homologous recombination. Transformants were selected for growth on SDC-his plates and then tested by Western blotting for the expression of the ProtA-Nup188p fusion protein which was functional since it could complement the nic96pΔ525-839 mutant strain lacking the carboxy-terminal domain (Grandi, P., unpublished results).

Indirect Immunofluorescence Microscopy

For immunofluorescence, cells were grown to 0.5 OD_{600}, fixed in 2% formaldehyde, and spheroplasted as described earlier (Wimmer et al., 1992; Doye et al., 1994). Myc-tagged Nup188p was immunolocalized using a monoclonal anti-Myc antibody which was affinity purified from ascites on protein A–Sepharose, followed by goat anti–mouse IgG + IgM coupled to lissamine/rhodamine (Jackson ImmunoResearch Laboratories, Inc., West Grove, PA). DNA was visualized by staining with Hoechst 33258.

Thin Section and Freeze/Fracture Electron Microscopic Analysis of Yeast Cells

All electron microscopic techniques were performed as described earlier (Doye et al., 1994). For statistical evaluation of the EM data, the number of NPCs counted in 15 different nuclei of each experiment was related to the length of the nuclear envelope (thin section EM) or nuclear surface (freeze/fracture EM). Nuclear envelope length and surface areas were determined using the square grid system described in (Mutvei et al., 1992).

Standard errors of the mean were calculated with the help of the EXCEL statistics program.

Results

Thermosensitive nic96-1 Cells Exhibit a Decrease in Nuclear Pore Density when Shifted to the Nonpermissive Condition

The role of the various Nic96p domains for cell viability and interaction with other NPC constituents was previously analyzed by a mutational analysis (Grandi et al., 1995*b*). Whereas the amino-terminal domain directly binds to the Nsp1p complex, the function of the essential central domain and the nonessential carboxy-terminal domain remained unclear (Grandi et al., 1995*b*). Two thermosensitive mutations mapping in the central Nic96p domain, *nic96-1* and *nic96-2*, were obtained which were impaired neither in the interaction with the core nucleoporin complex nor in uptake of a nuclear reporter protein or nuclear poly(A)$^+$ export (Grandi et al., 1995*b*) (Fig. 1 *A*). For further analysis, we concentrated on the *nic96-1* mutant, because it exhibits a more pronounced ts phenotype as compared with the *nic96-2* allele (Fig. 1, *B* and *C*). Accordingly, nic96-1 cells grew only slightly more slowly than NIC96$^+$ cells at 23°C, but stopped growth after shifting them for 7–8 h to 37°C which corresponds to 2–3 further cell divisions (Fig. 1 *B*). In contrast, nic96-2 cells grew well at 30°C, but slowly at 23°C, and showed a later growth arrest at 37°C (data not shown) and impaired cell growth at 23°C (Fig. 1 *B*). In the *nic96-1* allele, two point mutations, the changes of proline 332 located within an essential stretch of 20 uncharged amino acids to leucine, and of leucine at position 260 to proline, contribute to the ts phenotype, since their separation causes loss of thermosensitivity (data not shown).

Thin sectioning electron microscopy was performed with nic96-1 cells grown either at 23°C or shifted for 5 h to 37°C (Fig. 2 *A*). No gross ultrastructural changes of the nuclear membrane were seen in the mutant and abnormal structures such as nuclear envelope herniations and NPC clustering that were observed in several other nucleoporin mutants (Wente and Blobel, 1993; Doye et al., 1994; Gorsch et al., 1995; Wente and Blobel, 1994) were also not evident. However, the frequency with which nuclear pores were seen within the double nuclear membrane of nic96-1 cells was significantly reduced when the cells were grown for 5 h at 37°C as compared with room temperature growth (Fig. 2 *A*); accordingly, the nuclear membrane inspected on a given electron micrograph was often devoid of nuclear pores (data not shown). The few remaining nuclear pores that could be detected in the mutant cells, however, revealed a normal appearance at the level of electron microscopy (Fig. 2 *A*). We performed a statistical analysis to determine the number of nuclear pores within a given nuclear envelope segment of wild-type cells and mutant cells grown at 23°C and shifted for 5 h to 37°C (Table II). This revealed that there is about a three- to fourfold reduction of nuclear pores per unit nuclear membrane length at restrictive as compared with permissive temperature in nic96-1 cells, whereas the number of nuclear pores did not change in wild-type cells upon temperature shift. A similar reduction in nuclear pore density was also found for the

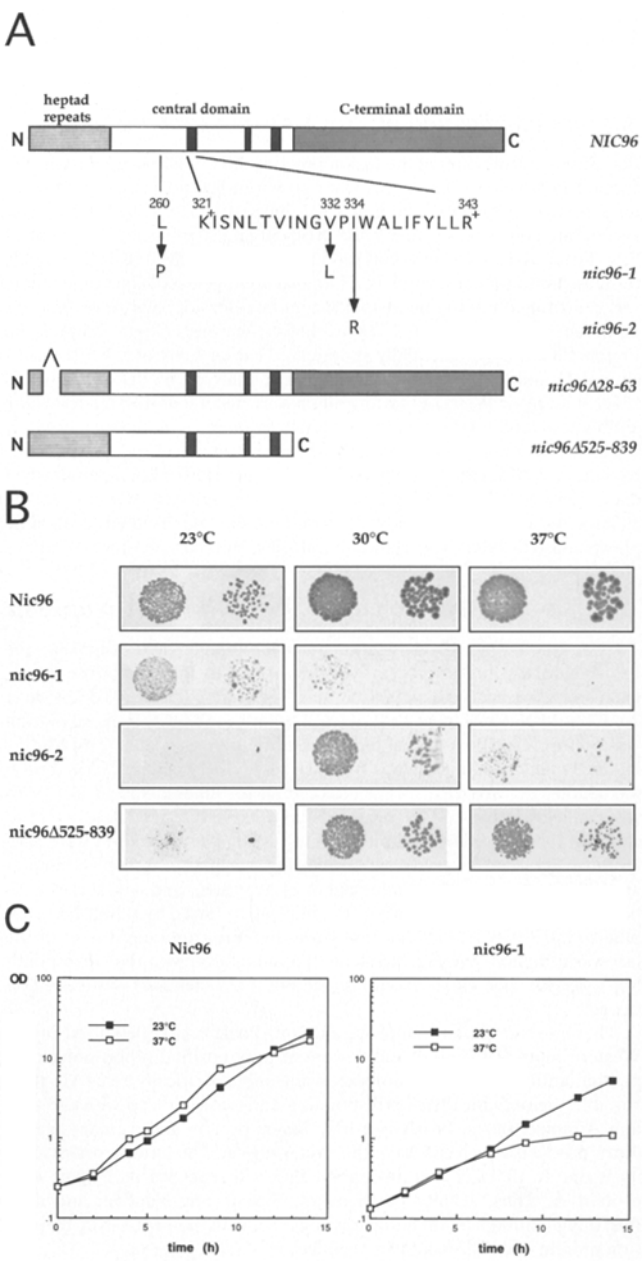

Figure 1. Characterization of *NIC96* mutant alleles. (*A*) Schematic representation of *NIC96* wild-type and mutant alleles. The amino acid sequence of one of the three longer stretches of uncharged amino acids found in the central domain (*dark boxes*) is drawn and the position and nature of the point mutations in nic96-1 and nic96-2 are indicated. (*B*) Growth of wild-type Nic96 and mutant nic96-1, nic96-2, and nic96Δ525-839 strains at different temperatures. Precultures of the indicated strains were diluted in liquid YPD medium and equivalent amounts of cells (undiluted or 1/10 diluted) were spotted onto YPD plates. Plates were incubated for 3 d at 23, 30, and 37°C, respectively. (*C*) Growth curves of wild-type Nic96 and temperature-sensitive nic96-1 strains in YPD liquid medium at 23°C (*filled squares*) or 37°C (*open squares*). Cell growth was followed by measuring the optical density at 600 nm (*OD*).

nic96-2 strain (data not shown). In contrast, the number of nuclear pores was not reduced in the NH_2-terminally truncated nic96Δ28-63 mutant grown at 37°C which is also thermosensitive for growth at 37°C and was shown to be

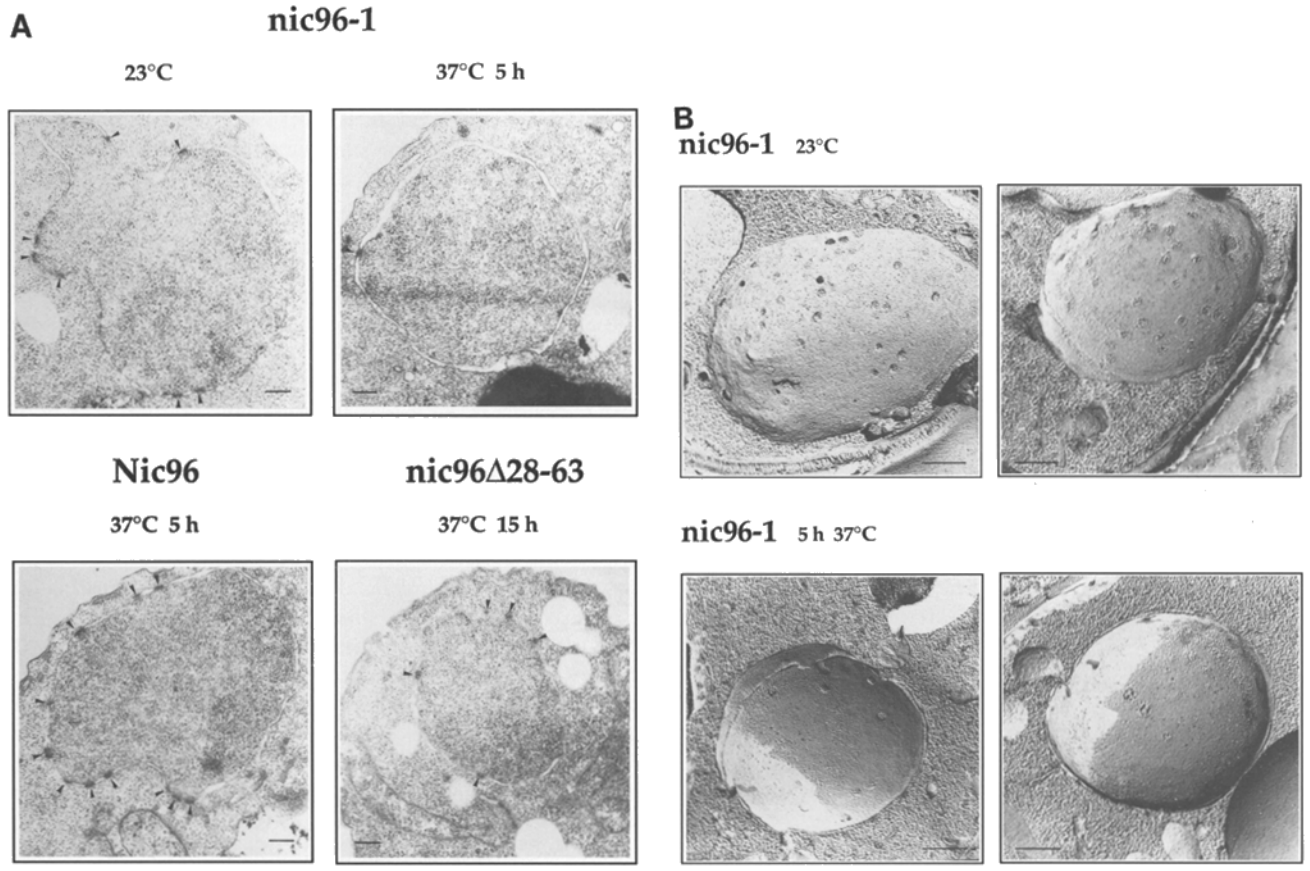

Figure 2. nic96-1 mutant cells have fewer nuclear pores at the restrictive temperature as revealed by EM analysis. (*A*) Thin section EM. Nic96 wild-type, nic96-1, and nic96Δ28-63 strains were grown at 23 or 37°C for the time indicated; cells were fixed and processed as described under Materials and Methods. Nuclear pore complexes are marked by arrowheads. Bars, 200 nm. (*B*) Freeze/fracture electron microscopy. nic96-1 cells were grown at 23°C or shifted for 5 h to 37°C. Cells were frozen and replicas were made as described under Materials and Methods. In nic96-1 cells grown at 37°C, large areas of the nuclear envelope are devoid of nuclear pores. Bars, 0.5 μm.

impaired in the interaction with the Nsp1p-containing core complex and uptake of a nuclear reporter protein (Grandi et al., 1995*b*).

These results were qualitatively confirmed by freeze/fracture electron microscopical analysis. Large nuclear membrane areas of nic96-1 cells grown for 5 h at 37°C were devoid of NPCs. At the permissive temperature the density of nuclear pores was similar to that in wild-type or nic96Δ28-63 cells grown at the restrictive temperature (Fig. 2 *B*; data not shown). Accordingly, the statistical analysis of these EM micrographs revealed a nuclear pore density of 9.87 pores/μm^2 nuclear surface at 37°C in NIC96$^+$ cells, and 2.77 pores/μm^2 in nic96-1 cells grown at restrictive temperature. The pore density in nic96-1 cells grown at the permissive temperature was with 6.02 pores/μm^2 already reduced relative to wild-type cells (Table II). In accordance with the EM data from the thin section analysis, the amino-terminally truncated nic96Δ28-63 mutant had a

Table II. Quantitation of Nuclear Pores in Nic96 Wild-type and Mutant Cells as Revealed by Thin Section and Freeze/Fracture Electron-Microscopic Analysis

Strain	Temp	Time	Thin section EM Pores/nuclear membrane length	Freeze/fracture EM Nuclear pores/nuclear surface
		h	μm^{-1}	μm^{-2}
Nic96	23°C		0.62 ± 0.05	ND
	37°C	5	0.63 ± 0.06	9.87 ± 0.65
nic96-1	23°C		0.53 ± 0.04	6.02 ± 0.44
	37°C	1	ND	6.34 ± 0.63
	37°C	5	0.14 ± 0.01	2.77 ± 0.32
nic96Δ28-63	23°C		0.79 ± 0.07	ND
	37°C	15	0.76 ± 0.05	8.66 ± 0.37

Nuclear pores of 15 individual nuclei from each experiment were counted, and the nuclear envelope length (thin sections) or surface (freeze/fracture) was determined (see Materials and Methods). Accordingly, results are given as pores/μm nuclear membrane length and pores/μm^2 nuclear surface, respectively. Errors are given as standard errors of the mean.

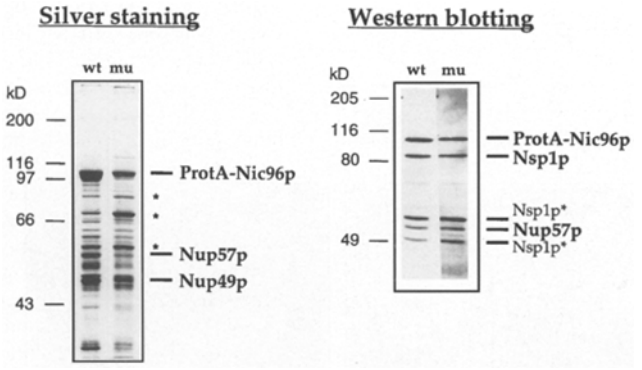

Figure 3. Affinity purification of ProtA-Nic96p and ProtA-nic96-1p. Cell lysates derived from ProtA-Nic96 (*wt*) and ProtA-nic96-1 (*mu*) strains grown at 23°C were applied onto an IgG-Sepharose column, and eluates were analyzed by SDS-9% PAGE followed by Silver staining and Western blotting, respectively. In the silver-stained gel (*left*), the positions of the fusion protein, Nup57p, and Nup49p are indicated. Prominent degradation products of the fusion proteins are marked by stars. The Western blot (*right*) was sequentially decorated with rabbit IgG coupled to HRP, anti-Nup57p, and anti-Nsp1p antibodies to detect the positions of the fusion protein, Nsp1p, and Nup57p; degradation products of Nsp1p are marked by stars. The position of molecular weight standard proteins is indicated.

normal density of 8.66 pores/μm^2 when grown at 37°C. Since in the freeze/fracture EM analysis no evidence was obtained that NPCs cluster in the nic96-1 cells, the apparent disappearance of NPCs from the nuclear envelope must be due to an overall decrease in nuclear pore density. In conclusion, these results suggest that the central domain of Nic96p is required to establish a normal nuclear pore density within the yeast nuclear membrane.

Affinity Purification of Wild-type and Mutant Nic96p from Whole Cell Lysates

To investigate whether the mutated Nic96 protein encoded by *nic96-1* is impaired in its interaction with other components of the NPC, an epitope-tagged form, ProtA-nic96-1p, was expressed in the *nic96*-disrupted strain. ProtA-nic96-1p and, for comparison, wild-type ProtA-Nic96p, were affinity purified under nondenaturing conditions by IgG-Sepharose chromatography (Fig. 3 *A*). This analysis confirmed the previous finding that nic96-1p still can associate with the core complex consisting of Nsp1p, Nup57p, and Nup49p (see also Grandi et al., 1995*b*). However, purification of ProtA-tagged nic96-1p or wild-type Nic96p showed that either fusion protein was in excess in the eluate as compared with the nucleoporins Nup57p, Nup49p, and Nsp1p. The nature of the bands in the 150–200 kD region associated with both mutant and wild-type Nic96p is currently under investigation (Fig. 3 *A*, silver staining; see also later). Since isolated ProtA-nic96-1p was apparently more susceptible to proteolysis during biochemical purification (see also Fig. 3 *A*, silver staining), we analyzed the stability of both wild-type and mutant fusion proteins in the cells when shifted to the restrictive temperature. In vivo, there was no obvious decrease in the amount of ProtA-nic96-1p as compared with wild-type ProtA-Nic96p within the first 5 h after shift to 37°C, a time point at which nic96-1 cells were already impaired in NPC biogenesis (data not shown). In conclusion, the mutations in the central domain of nic96-1p neither cause thermoinstability of the protein nor impair interaction with the Nsp1p core complex.

Identification of a Novel Nuclear Pore Protein Nup188p Via its Allele-specific Interaction with the Carboxy-terminal Domain of Nic96p

By biochemical analysis, no other prominent proteins than Nup49p, Nup57p, and Nsp1p copurified with Nic96p (see

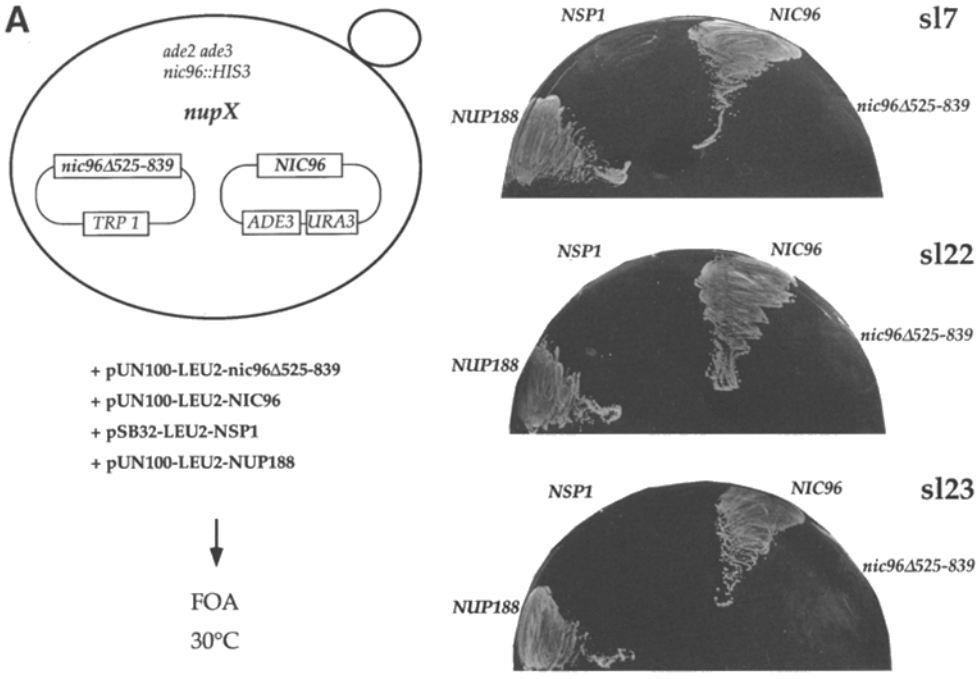

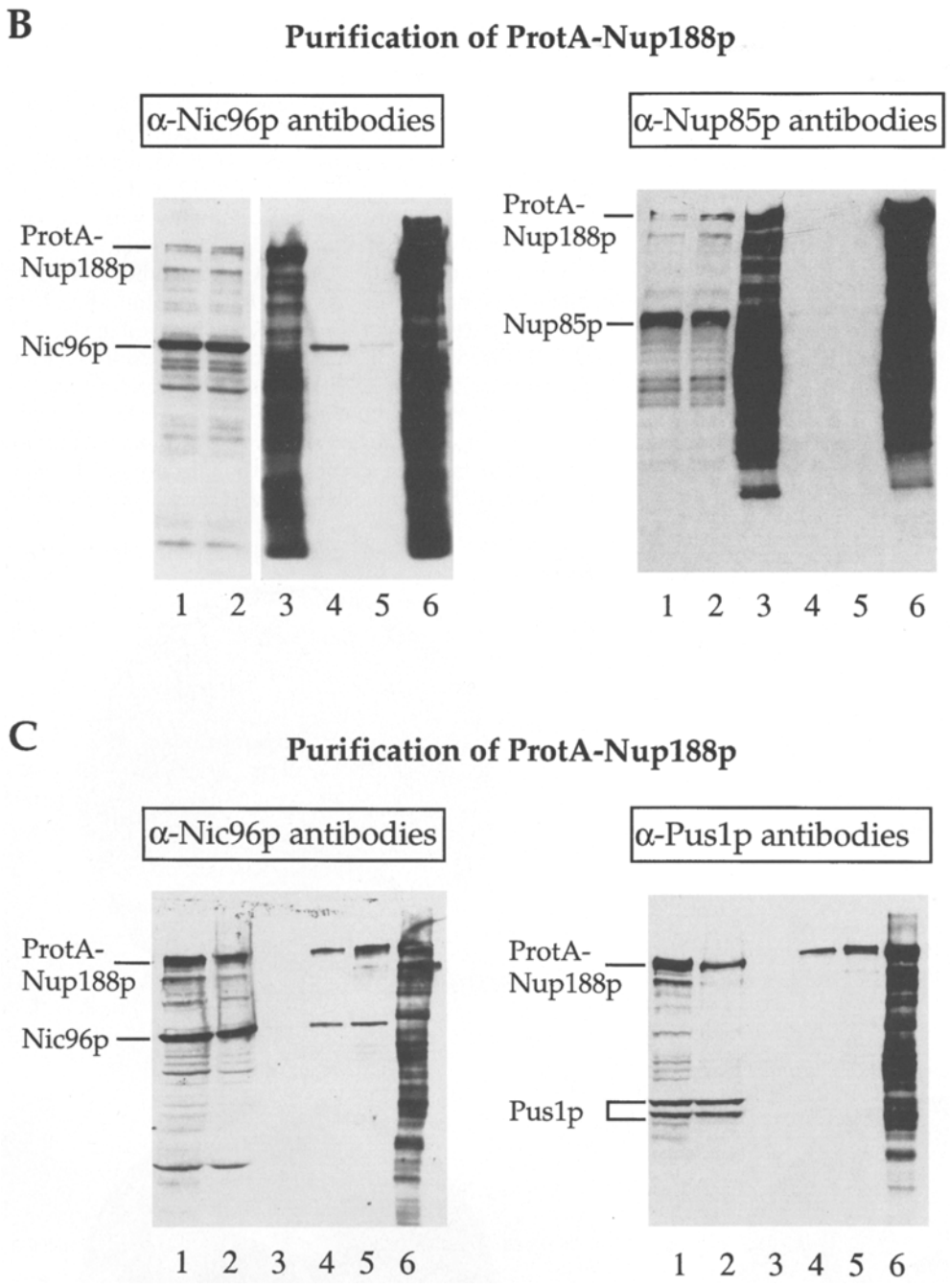

Figure 4. Interaction between Nup188p and Nic96p. (*A*) Three synthetic lethal mutants of the *nic96Δ525-839* allele were complemented by the *NUP188* gene. Isolation of synthetic lethal mutants of *NIC96*, using the *nic96Δ525-839* allele in a red/white colony sectoring assay was done as described under Materials and Methods. Three sl mutants sl7, sl22, and sl23 most likely carried mutations in the *NUP188* gene, since growth on 5-FOA plates was restored by either *NIC96* wild-type or *NUP188*-containing plasmids, but not by the *nic96Δ525-839* allele or *NSP1*. To test for complementation, transformants were first grown on selective medium lacking leucine and tryptophane (see schematic drawing on left), before loss of the *URA3*-containing plasmid carrying *NIC96* was induced on 5-FOA plates for 3 d at 30°C (*right*). (*B* and *C*) Nic96p is associated with purified ProtA-Nup188p. Western blot (*B*) ProtA-Nup188p was affinity purified on a IgG-Sepharose column and the bound proteins were eluted by acidic pH (lane *3*) or by increasing concentrations of $MgCl_2$ (lane *4*, 0.6 M $MgCl_2$; lane *5*, 2 M $MgCl_2$; lane *6*, 4.5 M $MgCl_2$) as described under Materials and Methods. All fractions including the load fraction (lane *1*), flow through fraction (lane *2*) and eluate fractions were analyzed by SDS-PAGE and Western blotting using affinity purified anti-Nic96p and anti-Nup85p antibodies. Note that the IgGs of anti-Nic96p/Nup85p antibodies also stain the ProtA moiety of ProtA-Nup188p as well as the many breakdown products of ProtA-Nup188p. The reason why in lanes *3* and *6* so many protein bands are visible is due to the fact that the affinity purified anti-Nic96p and anti-Nup85 antibodies not only specifically react via their variable region with Nic96p and Nup85p, respectively, but also with the protein A moiety of the ProtA-Nup188p fusion protein and its many breakdown products which still have the ProtA tag on. The latter cross-reactivity is due to the fact that any rabbit IgG will react via its F_c part with protein A. Western blot (*C*) ProtA-Nup188p was affinity purified on a IgG-Sepharose column and the bound proteins were eluted as described in the figure legend 4 *B*. On this blot, also the wash fraction (lane *3*) was included and the blot was exposed to a shorter extent to better see the protein bands. Fractions were analyzed by SDS-PAGE and Western blotting using affinity purified anti-Nic96p and Pus1p antibodies. Pus1p is an intranuclear protein (Simos et al., 1996) and served as a negative control. 1, load fraction; 2, flow through fraction; 3, wash fraction; 4, 5, and 6, $MgCl_2$-induced eluate fractions (lane *4*, 0.6 M $MgCl_2$; lane *5*, 2 M $MgCl_2$; lane *6*, 4.5 M $MgCl_2$). Note that in this experiment a small fraction of the fusion protein was also eluted from the column between 0.6 and 2 M $MgCl_2$ (see also Siniossoglou et al., 1996).

also Fig. 3 *A*). Since the amino-terminal domain, which mediates the binding to these core complex nucleoporins, is dispensable for cell growth (Grandi et al., 1995*b*), Nic96p should be linked via its central and carboxy-terminal domain to other NPC proteins. To identify these nuclear pore proteins which interact with this part of Nic96p, we performed sl screens with *nic96* mutants alleles mapping in these domains (Grandi et al., 1995*b*), using a red/white colony sec-

toring assay as described earlier (Wimmer et al., 1992). In one screen, we used a *nic96* allele in which the carboxy-terminal domain was completely missing (nic96pΔ525-839). This allele allows the cells to grow normally at 30 and 37°C, but at 23°C a slightly reduced growth rate was noticed (Fig. 1 *B*). From this screen, seven nonsectoring red mutants were obtained (see Materials and Methods). Subsequent transformation with plasmids carrying either wild-type *NIC96* or mutant *nic96Δ525-839* alleles revealed that three strains, sl7, sl22, and sl23, fulfilled all criteria of being synthetically lethal with *nic96Δ525-839*, since wild-type *NIC96* restored red/white colony sectoring (data not shown) and growth on 5-FOA plates, whereas the *nic96Δ525-839* allele did not (Fig. 4 *A*). To find out whether any of these sl strains is complemented by one of the already cloned yeast nucleoporins, cells were transformed with plasmids carrying different nucleoporin genes (see Materials and Methods). All three sl mutants were complemented by a novel gene, designated *NUP188*, which was independently isolated in our laboratory through its genetic interaction with *NSP1* (see also Materials and Methods). All the other nucleoporin genes tested, including *NSP1*, could not complement the nic96 sl mutants. Thus, it is likely that sl7, sl22, and sl23 acquired mutations in the *NUP188* gene (these sl alleles will be called *nup188-7*, *nup188-22*, and *nup188-23*) which specifically cause synthetic lethality with the carboxy-terminally truncated *nic96Δ525-839* allele.

To investigate whether the observed synthetic lethality is allele specific, we tested other *nic96* mutant alleles for complementation of the sl phenotype observed in sl7, sl22, and sl23 (Fig. 5). Strikingly, sl7 and sl23 were only synthetically lethal with *nic96Δ*525-839, but not with thermosensitive *nic96-1*, *nic96-2*, and *nic96Δ28-63* alleles (Fig. 5, *right*), showing a strict allele specificity towards *nic96* mutant genes which lack the carboxy-terminal domain. In contrast, the *nup188-22* allele causes a sl phenotype also with

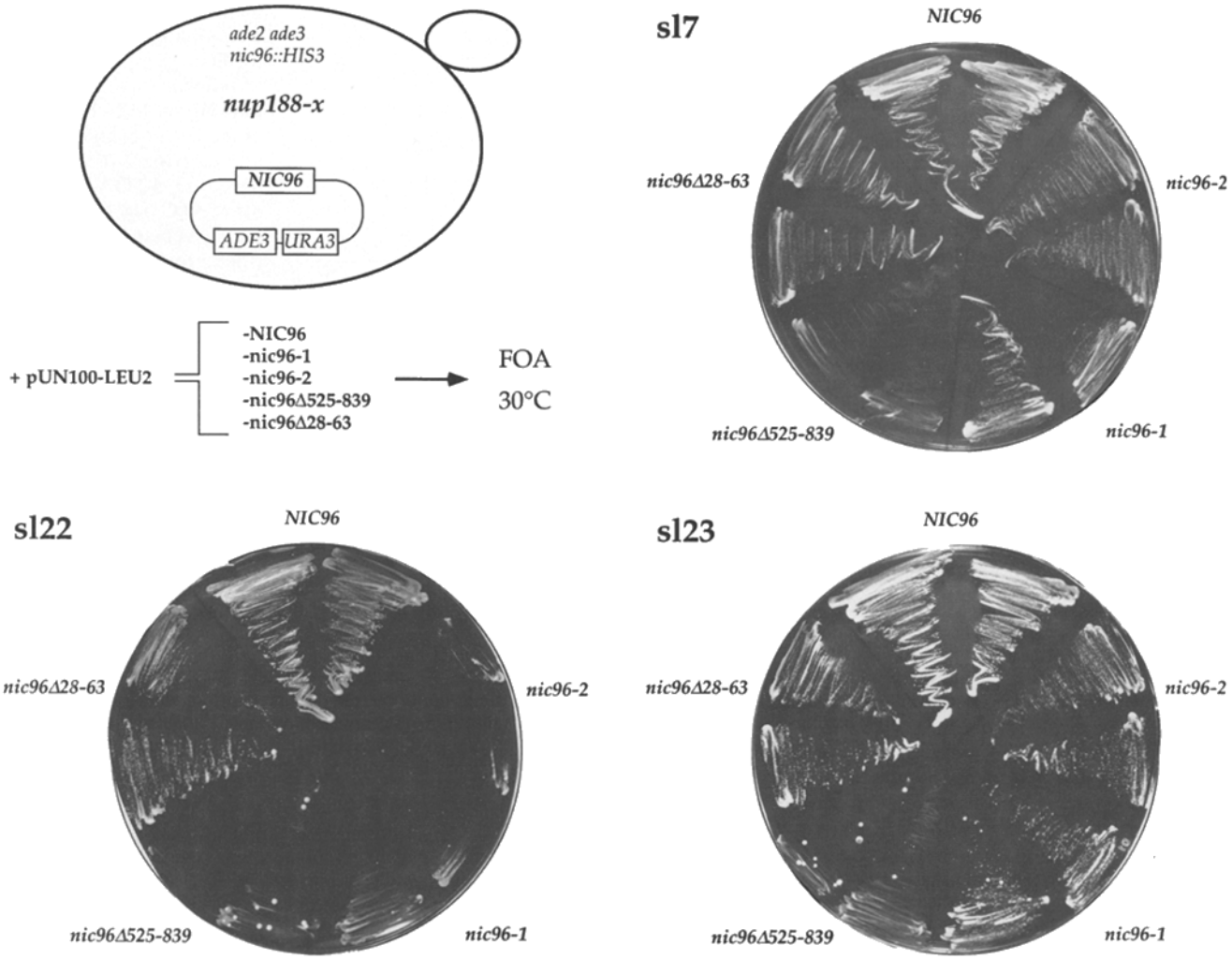

Figure 5. Allele-specific synthetic lethality between *nic96* and *nup188*. Strains sl7, sl22, and sl23, harboring a *URA3/ADE3*-containing plasmid carrying *NIC96* wild-type were transformed with *nic96Δ525-839*, *nic96-1*, *nic96-2*, and *nic96Δ28-63* mutant alleles, present on a single copy number *LEU2*-containing ARS/CEN plasmid (see also Materials and Methods). Loss of the *URA3*-containing plasmid carrying *NIC96* in the transformed strains was induced by plating cells on 5-FOA–containing plates for 5 d at 30°C. The *NIC96* wild-type and *nic96Δ28-63* alleles allowed all three sl strains to grow on 5-FOA plates (two individual transformants were plated), whereas the *nic96Δ525-839* allele did not (the few growing colonies observed in sl22 and sl23 could be revertants). sl7- and sl23-derived transformants were also complemented by *nic96-1* and *nic96-2* thermosensitive alleles. In contrast, sl22 failed to grow on 5-FOA also with *nic96-1* and *nic96-2*.

the *nic96-1* and *nic96-2* alleles (Fig. 5, *lower left*); however, this genetic interaction seems to be weaker, since very slow growth of the corresponding strains was noticed, resulting in the formation of microcolonies on 5-FOA plates. Interestingly, none of the three *nup188* alleles is synthetically lethal in combination with the *nic96Δ28-63* allele. All these data suggest a functional linkage between Nup188p and the carboxy-terminal and the central domain of Nic96p and no interaction between Nup188p and the amino-terminal domain of Nic96p (see also Discussion).

Affinity Purification of ProtA-Nup188p and Association with Nic96p

To test whether Nup188p is also physically associated with Nic96p, Nup188p was tagged with two IgG-binding sequences derived from *Staphylococcus aureus* protein A and affinity purified under nondenaturing conditions by IgG-Sepharose chromatography. Since the nic96pΔ525-839 mutant strain carrying *ProtA-NUP188* integrated at the authentic *NUP188* gene locus was viable and grew normally, ProtA-Nup188p was functional (see also Materials and Methods). The IgG-Sepharose column containing bound ProtA-Nup188p was first extensively washed with a 200-fold bead volume to remove unspecifically bound proteins (see Materials and Methods), before Nic96p associated with ProtA-Nup188p was eluted with increasing concentrations of $MgCl_2$. The fractions were analyzed for the presence of Nic96p, as well as Nup85p (another nucleoporin) and Pus1p (an intranuclear protein; Simos et al., 1996), by SDS-PAGE and Western blotting using affinity purified antibodies (Fig. 4, *B* and *C*). We recently showed that nucleoporins associated with a given ProtA-tagged nuclear pore protein immobilized on a IgG-Sepharose column can be eluted from the column by increasing concentrations of $MgCl_2$ (Siniossoglou et al., 1996). When tested in a similar way, a fraction of Nic96p is associated with ProtA-Nup188p (Fig. 4, *B* and *C*). Accordingly, Nic96p was not found in the wash fraction, but could be eluted from the IgG-sepharose column between 0.6 and 2 M $MgCl_2$. In contrast, the ProtA-Nup188p and its many proteolytic breakdown products (Nup188p is very sensitive to proteolysis after cell lysis) were mainly released from the column at 4.5 M $MgCl_2$. When the 0.6 and 2 M $MgCl_2$ eluates were analyzed for the presence of another NPC protein (e.g., Nup85p; Siniossoglou et al., 1996) or an intranuclear protein (e.g., Pus1p; Simos et al., 1996), no significant association with ProtA-Nup188p was detected (Fig. 4, *B* and *C*).

Disruption of the NUP188 Gene Causes Structural Abnormalities within the Nuclear Envelope

The *NUP188* gene which was initially isolated through its genetic interaction with a thermosensitive *nsp1* allele (see Materials and Methods) encodes the as yet largest yeast nuclear pore protein with a molecular mass of 188 kD (Fig. 6). Comparison of the Nup188p amino acid sequence with the sequences present in the data libraries did not reveal a significant homology to known proteins showing that Nup188p is a novel protein. Its subcellular location was analyzed by performing indirect immunofluorescence with a yeast strain expressing a triple myc-tagged Nup188p fusion protein.

```
   1 MATPSFGNSS PQLTFTHVAN FMNDAAADVS AVDAKQLAQI RQFLKANKTN
  51 LIESLNTIRQ NVTSSGDHNK LRSTIANLLQ INVDNDPFFA QSEDLSHAVE
 101 FFMSERSSRL HIVYSLLVNP DIDLETYSFI DNDRFNVVGK LISIISSVIQ
 151 NYDIITASSL AHDYNNDQDM FTIVSLVQLK KFSDLKFILQ ILQILNLMIL
 201 NTKVPVDIVN QWFLQYQNQF VEFCRNINST DKSIDTSSLQ LYKFQNFQDL
 251 SYLSETLISR ISSLFTITTI LILGLNTSIA QFDIQSPLYM DTETFDTVNS
 301 ALENDVATNI VNEDPIFHPM IHYSWSFILY YRRALQSSES FDDSDITKFA
 351 LFAESHDVLQ KLNTLSEILS FDPVYTTVIT VFLEFSLNFI PITASTSRVF
 401 AKIISKAPEQ FIENFLTNDT FEKKLSIIKA KLPLLNESLI PLINLALIDT
 451 EFANFELKDI CSFAVTKSSL NDLDYDLIAD TITNSSSSSD IIVPDLIELK
 501 SDLLVAPPLE NENSNCLLSI PKSTKGKILT IKQQQQQQQQ QNGQQPPTTS
 551 NLIIFLYKFN GWSLVGRILQ NLLHSYMEKG TQLDDLQHEL MISIIKLVTN
 601 VVDPKTSIEK SSEILSYLSN SLDTSASTIN GASIIQVIFE IFEISLQRKD
 651 YTSIVQCCEF MTMLTPNYLH LVSSYLNKSD LLDKYGKTGL SNMILGSVEL
 701 STGDYTFTIQ LLKLTKVFIR ESLSLKNIHI SKRSKIDIIN KLILHAIHIF
 751 ESYYNWKYNN FLQKFEIAFH LTLIFYDVLH DVFTINPHQK DQLIISSSAN
 801 KLLQLFLTPM DSIDLAPNTL TNILISPLNT TTKILGDKIL GNLYSKVMNN
 851 SFKLCTLLIA IRGSNRDLKP SNLEKLLFIN SSKLVDVYTL PSYVHFKVQI
 901 IELLSYLVEA PWNDDYPFLL SFLGEAKSMA FLKEVLSDLS SPVQDWNLLR
 951 SLYIFFTTLL ESKQDGLSIL FLTGQFASNK KINDESSIDK KSSILTVLQK
1001 NSLLLDSTPE EVSCKLLETI TYVLNTWTNS KIFIKDPKFV NSLLAKLKDS
1051 KKLFQKKENL TRDETVSLIK KYKLISRIVE IFALCIYNST DSNSEILNFL
1101 NQEDLFELVH HFFQIDGFNK TFHDELNLKF KEKWPSLELQ SFQKIPLSRI
1151 NENENFGYDI PLLDIVLKAD RSWNEPSKSQ TNFKEEITDA SLNLQYVNYE
1201 ISTAKAWGAL ITTFVKRSTV PLNDGFVDLV EHFLKLNIDF GSDKQMFTQI
1251 YLERIELSFY ILYSFKLSGK LLKEEKIIEL MNKIFTIFKS GEIDFIKNIG
1301 KSLKNNFYRP LLRSVLVLLE LVSSGDRFIE LISDQLLEFF ELVFSKGVYL
1351 ILSEILCQIN KCSTRGLSTD HTTQIVNLED NTQDLLLLLS LFKKITNVNP
1401 SKNFNVILAS SLNEVGTLKV ILNLYSSAHL IRINDEPILG QITLTFISEL
1451 CSIEPIAAKL INSGLYSVLL ESPLSVAIQQ GDIKPEFSPR LHNIWSNGLL
1501 SIVLLLLSQF GIKVLPETCL FVSYFGKQIK STIYNWGDNK LAVSSSLIKE
1551 TNQLVLLQKM LNLLNYQELF IQPKNSDDQQ EAVELVIGLD SEHDKKRLSA
1601 ALSKFLTHPK YLNSRIIPTT LEEQQQLEDE SSRLEFVKGI SRDIKALQDS
1651 LFKDV*
```

Figure 6. Amino acid sequence of Nup188p. The cloning and sequence analysis of the genomic DNA encoding Nup188p is described under Materials and Methods. Two longer stretches of uncharged amino acids in the amino-terminal part of Nup188p and a polyglutamine track are underlined. These sequence data are available from EMBL/GenBank/DDBJ under accession number X90580.

The observed punctate staining of the nuclear envelope indicates that Nup188p is a nuclear pore protein (Fig. 7). This was independently found by Nehrbass et al. (see accompanying paper) who identified Nup188p as an abundant nuclear pore protein in the highly purified yeast NPC preparation (Rout and Blobel, 1993). To determine whether Nup188p is essential for cell growth, the *NUP188* gene was disrupted in a diploid yeast strain by replacing about half of its coding sequence with the *HIS3* gene (see Materials and Methods). Sporulation of this strain followed by tetrad analysis yielded four viable spores at 23, 30, and 37°C which display a similar growth rate as compared

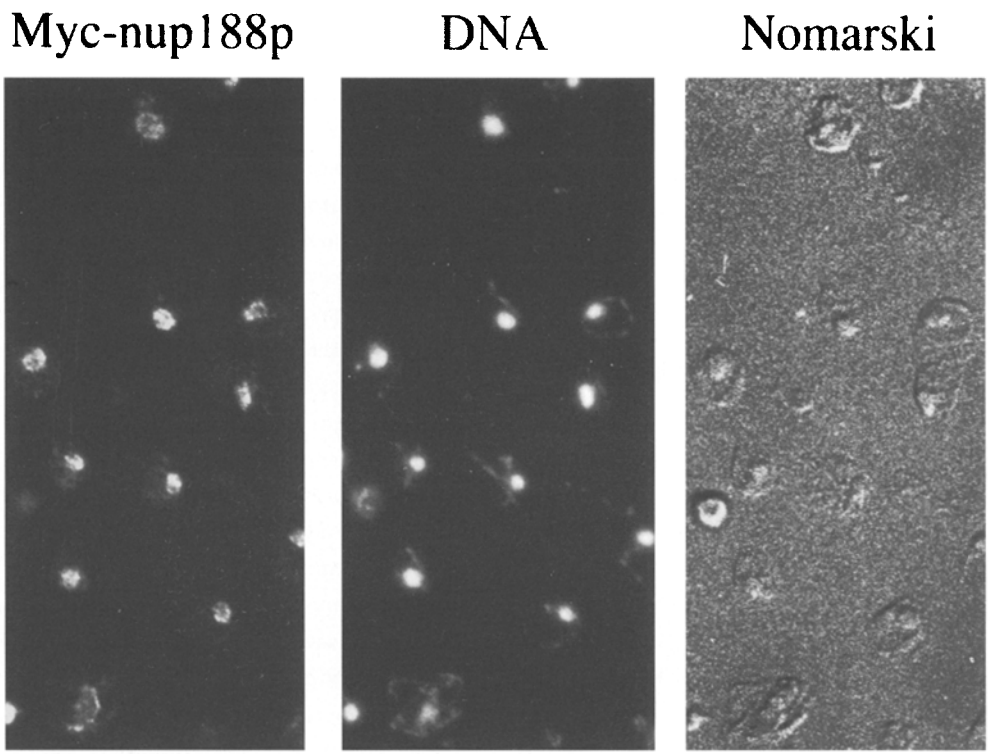

Figure 7. Subcellular localization of Myc-Nup188p as revealed by indirect immunofluorescence microscopy. A punctate staining of the nuclear envelope is observed in Myc-Nup188 cells using monoclonal anti-myc antibodies followed by goat anti-mouse IgG+IgM coupled to Lissamine/Rhodamine. Cells were also stained with Hoechst 33258 for DNA and viewed by Nomarski optics.

to NUP188$^+$ cells. This shows that *NUP188* is not essential for cell growth.

To find out whether the deprivation of Nup188p from the nuclear pores will cause ultrastructural perturbations of the nuclear envelope, electron microscopy of thin sectioned yeast cells carrying the disrupted *nup188::HIS3* allele was performed (Fig. 8). nup188$^-$ cells grown at either 23 or 37°C, although still having typical NPCs, often reveal striking structural defects of the nuclear envelope. These distortions resemble the herniations of the nuclear envelope over the nuclear pore complexes which were initially described for the *nup116* disruption mutant (Wente and Blobel, 1993). This includes individual blisters with an NPC-like structure at the base, or multiple herniations that are surrounded by a common outer nuclear membrane seal; some of these blisters can be detached completely from the inner nuclear membrane thus forming a kind of inner nuclear membrane vesicle between the widely separated outer and inner nuclear membranes (Fig. 8, *arrows*); however, serial thin sections would be needed to precisely describe these structures. In addition, nup188$^-$ cells frequently reveal electron-dense material resembling in size the electron-dark material of normal NPCs, but these structures are only attached to the inner nuclear membrane which is not fused to the outer nuclear membrane. These could be sites at which NPC biogenesis started, but was not completed due to the lack of Nup188p. Other morphological abnormalities such as NPC clustering or the successive herniations of the nuclear membrane forming grapelike structures as seen in nup133$^-$ cells (Doye et al., 1994; Gorsch et al., 1995) and nup145ΔN cells (Wente and Blobel, 1994), respectively, were not observed in nup188$^-$ cells.

In summary, although *NUP188* is not essential for cell growth, it is required for proper nuclear envelope/nuclear

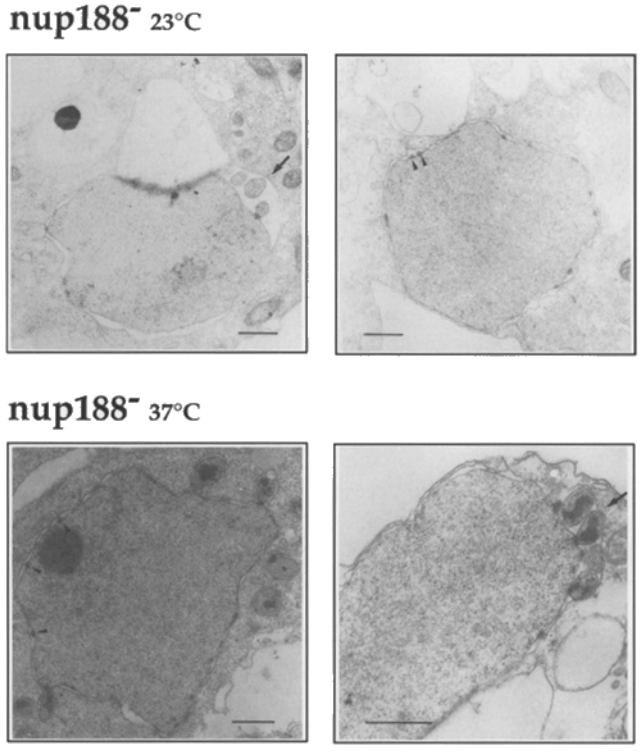

Figure 8. nup188$^-$ cells exhibit several morphological abnormalities in the nuclear membrane. nup188 disrupted cells were grown to the early logarithmic phase at 23 or 37°C before processing for thin section electron microscopic analysis as described under Materials and Methods. Arrowheads indicate electron-dense NPC-like structures attached only to the inner nuclear membrane; arrows point to large blisters of the nuclear membrane filled with electron-dense material. Bars, 0.5 μm.

pore biogenesis. This suggests that Nup188p could play a role in correctly anchoring the NPCs within the nuclear membrane (see also Discussion).

Discussion

This work provides evidence that Nic96p performs several important functions at the NPC. Whereas its amino-terminal domain which exhibits heptad repeats was already shown to bind to the Nsp1p/Nup49p/Nup57p nucleoporin complex (Grandi et al., 1995*b*), the central- and carboxy-terminal domain of Nic96p in conjunction with other NPC proteins may play other roles in NPC organization. We have found that thermosensitive mutations within the essential central domain of Nic96p inhibit nuclear pore formation and both the central- and COOH-terminal domains are linked to another NPC component Nup188p which itself is required for normal nuclear membrane/nuclear pore biogenesis.

In the nic96-1 mutant, two amino acid exchanges mapping in the central domain cause a significant reduction in nuclear pore density. Since this decrease is only observed when cells were allowed to divide at the nonpermissive temperature (e.g., for 5 h), we believe that only the formation of new nuclear pores is impaired and the preexisting pores become successively diluted by cell and nuclear division. It is not clear why the nic96-1 cells stop growing upon shift to 37°C. Since the remaining nuclear pores seem to be still competent for nucleocytoplasmic transport, because uptake of a nuclear reporter protein (Grandi et al., 1995*b*) or poly(A)$^+$ RNA export were apparently not impaired, it thus could be that cells stopped their growth in response to a reduced NPC density, or to other defects which are not yet known.

In higher eukaryotes, immunodepletion of nucleoporin p62 from *Xenopus* egg extracts led to inhibition of nuclear pore assembly, but a double nuclear membrane still formed (Dabauvalle et al., 1990). Similar results were obtained when the *Xenopus* egg extract used to study nuclear formation was depleted for wheat germ agglutinin binding proteins (Miller and Hanover, 1994). In yeast, a decrease in nuclear pores as well as inhibition of nuclear uptake of a reporter protein were observed upon transcriptional repression of *NSP1* (Mutvei et al., 1992). In contrast to these previous findings, inhibition of nuclear pore formation as described here did not require the complete removal of a nuclear pore protein from the cell or reconstitution extract, but two point mutations in the central domain of Nic96p were sufficient to establish such a phenotype. In contrast, point mutations in a Nsp1p mutant which cause a thermosensitive phenotype and inhibition of nuclear transport, did not inhibit NPC biogenesis at the nonpermissive temperature (Nehrbass et al., 1993).

To understand how Nic96p is involved in NPC biogenesis, it is important to identify its interacting components. So far, we could demonstrate that Nsp1p, Nup57p, and Nup49p are associated with Nic96p. We now have found that a novel nucleoporin Nup188p is functionally linked to the COOH-terminal and central domain of Nic96p. Thus, Nup188p is a promising candidate for an additional Nic96p-interacting protein. In fact, we could obtain biochemical evidence that Nic96p is associated physically with Nup188p. However, the amount of Nic96p attached to ProtA-Nup188p was only substoichiometric; this may reflect a less stable physical interaction between the two proteins, or only a pool of Nic96p is associated with Nup188p. Nup188p by itself is important for normal nuclear envelope formation and NPC structure, since a *nup188* disruption mutant, although viable, revealed several structural distortions of the nuclear membrane, the most prominent one being seals of the nuclear membrane over the NPC causing a nuclear envelope blistering phenotype. Nup188p, therefore, may be required for correct insertion and/or anchoring of NPCs at the pore membrane. A similar function was discussed for the yeast nucleoporin Nup116p, because disruption of its gene causes morphological defects strongly resembling those seen in nup188$^-$ cells (Wente and Blobel, 1993). nup145ΔN cells which, like nup188$^-$ cells, do not exhibit growth defects, display, in addition to herniations of the nuclear envelope, clustering of NPCs which often appear in grapelike structures (Wente and Blobel, 1994). The latter morphological abnormality is not observed in the nup188$^-$ cells. Accordingly, Nup188p does not seem to affect anchoring of NPCs to a matrix underlying the nuclear envelope, as was discussed for Nup145p and Nup133p (Doye et al., 1994; Wente and Blobel, 1994; Gorsch et al., 1995).

Sequence analysis of *NUP188* revealed neither striking homology to known proteins, nor diagnostic sequence motifs that could give clues to its function. Like Nup116p, Nup188p is not an integral pore membrane protein (Doye, V., unpublished data), although two longer stretches of uncharged amino acid residues can be found in the primary sequence (Fig. 6). Nup188p therefore may be a peripheral membrane protein. Interestingly, Nup188p is also functionally linked to Pom152p, a yeast nuclear pore membrane protein (Nehrbass et al., 1996; accompanying paper). Since mutations in both Nup188p and the Nic96p COOH-terminal domain lead to synthetic lethality with a thermosensitive *nsp1* allele (this study and Grandi et al., 1995*b*), all these proteins are somehow functionally linked to each other. One possibility is that Nic96p forms separate complexes, e.g., with the Nsp1p complex to dock peripheral repeat-containing nucleoporins at the NPC or with Nup188p to associate with distinct pore structures. Our future work will address the question of how Nic96p can perform these various roles at the NPC.

We thank Dr. Steve Kron (Whitehead Institute, MA) for providing the triple myc-tag and Elena Ikkonen (EMBL) for giving us the monoclonal anti-Myc antibody. We gratefully acknowledge Maria Ericson for help in electron microscopy, Dietlinde Schullerus for technical assistance, and Iain Mattaj and various members of the lab for their critical comments on the manuscript. We are also thankful to Drs. G. Blobel, U. Nehrbass, and R. Wozniak for communicating their data on Nic96p/Nup188p before publication.

E.C. Hurt received a grant from the Deutsche Forschungsgemeinschaft.

Received for publication 22 August 1995 and in revised form 24 February 1996.

References

Adam, E.J.H., and S.A. Adam. 1994. Identification of cytosolic factors required for nuclear location sequence-mediated binding to the nuclear envelope. *J. Cell Biol.* 125:547–555.

Bogerd, A.M., J.A. Hoffmann, D.C. Amberg, G.R. Fink, and L.I. Davis. 1994. *nup1* mutants exhibit pleiotropic defects in nuclear pore complex function. *J. Cell Biol.* 127:319–332.

Burke, B., and L. Gerace. 1986. A cell free system to study reassembly of the nuclear envelope at the end of mitosis. *Cell.* 44:639–652.

Buss, F., and M. Stewart. 1995. Macromolecular interactions in the nucleoporin p62 complex of rat nuclear pores: binding of nucleoporin p54 to the rod domain of p62. *J. Cell Biol.* 128:251–261.

Buss, F., H. Kent, M. Stewart, S.M. Bailer, and J.A. Hanover. 1994. Role of different domains in the self-association of rat nucleoporin p62. *J. Cell Sci.* 107: 631–638.

Dabauvalle, M.-C., and U. Scheer. 1991. Assembly of nuclear pore complexes in Xenopus egg extract. *Biol. Cell. (Ivry Sur Seine).* 72:25–29.

Dabauvalle, M.-C., K. Loos, and U. Scheer. 1990. Identification of a soluble precursor complex essential for nuclear pore assembly. *Chromosoma (Berl.).* 100:56–66.

Doye, V., and E.C. Hurt. 1995. Genetic approaches to nuclear pore structure and function. *Trends Genet.* 11:193–199.

Doye, V., R. Wepf, and E.C. Hurt. 1994. A novel nuclear pore protein Nup133p with distinct roles in poly $(A)^+$ RNA transport and nuclear pore distribution. *EMBO (Eur. Mol. Biol. Organ.) J.* 13:6062–6075.

Elledge, S.J., and R.W. Davis. 1988. A family of versatile centromeric vectors designed for use in the sectoring-shuffle mutagenesis assay in *Saccharomyces cerevisiae. Gene (Amst.).* 70:303–312.

Enenkel, C., G. Blobel, and M. Rexach. 1995. Identification of a yeast karyopherin heterodimer that targets import substrate to mammalian nuclear pore complexes. *J Biol. Chem.* 270:16499–16502.

Fabre, E., W.C. Boelens, C. Wimmer, I.W. Mattaj, and E.C. Hurt. 1994. Nup145p is required for nuclear export of mRNA and binds homopolymeric RNA in vitro via a novel conserved motif. *Cell.* 78:275–289.

Finlay, D.R., and D.J. Forbes. 1990. Reconstitution of biochemically altered nuclear pores: transport can be eliminated and restored. *Cell.* 60:17–29.

Finlay, D.R., E. Meier, P. Bradley, J. Horecka, and D.J. Forbes. 1991. A complex of nuclear pore proteins required for pore function. *J. Cell Biol.* 114:169–183.

Gorsch, L.C., T.C. Dockendorff, and C.N. Cole. 1995. A conditional allele of the novel repeat-containing yeast nucleoporin *RAT7/NUP159* causes both rapid cessation of mRNA export and reversible clustering of nuclear pore complexes. *J. Cell Biol.* 129:939–955.

Grandi, P., V. Doye, and E.C. Hurt. 1993. Purification of NSP1 reveals complex formation with 'GLFG' nucleoporins and a novel nuclear pore protein NIC96. *EMBO (Eur. Mol. Biol. Organ.) J.* 12:3061–3071.

Grandi, P., S. Emig, C. Weise, F. Hucho, T. Pohl, and E.C. Hurt. 1995*a*. A novel nuclear pore protein Nup82p which specifically binds to a fraction of Nsp1p. *J. Cell Biol.* 130:1263–1273.

Grandi, P., N. Schlaich, H. Tekotte, and E.C. Hurt. 1995*b*. Functional interaction of Nic96p with a core nucleoporin complex consisting of Nsp1p, Nup49p and a novel protein Nup57p. *EMBO (Eur. Mol. Biol. Organ.) J.* 14:76–87.

Greber, U.F., A. Senior, and L. Gerace. 1990. A major glycoprotein of the nuclear pore complex is a membrane-spanning polypeptide with a large luminal domain and a small cytoplasmic tail. *EMBO (Eur. Mol. Biol. Organ.) J.* 9:1495–1502.

Görlich, D., and E. Hartmann. 1995. A Ran-binding motif in nuclear pore proteins. *Trends Cell Biol.* 5:192–193.

Görlich, D., S. Prehn, R.A. Laskey, and E. Hartmann. 1994. Isolation of a protein that is essential for the first step of nuclear protein import. *Cell.* 79:767–778.

Grote, M., U. Kubitscheck, R. Reichelt, and R. Peters. 1995. Mapping of nucleoporins to the center of the nuclear pore complex by post-embedding immunogold electron microscopy. *J. Cell Sci.* 108:2963–2972.

Hallberg, E., R.W. Wozniak, and G. Blobel. 1993. An integral membrane protein of the pore membrane domain of the nuclear envelope contains a nucleoporin-like region. *J. Cell Biol.* 122:513–521.

Hurt, E.C. 1990. Targeting of a cytosolic protein to the nuclear periphery. *J. Cell Biol.* 111:2829–2837.

Izaurralde, E., J. Lewis, C. McGuigan, M. Jankowska, E. Darzynkiewicz, and I.W. Mattaj. 1994. A nuclear cap binding protein complex involved in pre-mRNA splicing. *Cell.* 78:657–668.

Kita, K., S. Omata, and T. Horigome. 1993. Purification and characterization of a nuclear pore glycoprotein complex containing p62. *J. Biochem. (Tokyo).* 113:377–382.

Li, O., C.V. Heath, D.C. Amberg, T.C. Dockendorff, C.S. Copeland, M. Snyder, and C.N. Cole. 1995. Mutation or deletion of the *Saccharomyces cerevisiae* RAT3/NUP133 gene causes temperature-dependent nuclear accumulation of poly $(A)^+$ RNA and constitutive clustering of nuclear pore complexes. *Mol. Biol. Cell.* 6:401–417.

Macaulay, C., E. Meier, and D.J. Forbes. 1995. Differential mitotic phosphorylation of proteins of the nuclear pore complex. *J. Biol. Chem.* 270:254–262.

Melchior, F., B. Paschal, J. Evans, and L. Gerace. 1993. Inhibition of nuclear protein import by nonhydrolyzable analogues of GTP and identification of the small GTPase Ran/TC4 as an essential transport factor. *J. Cell Biol.* 123: 1649–1659.

Miller, M.W., and J.A. Hanover. 1994. Functional nuclear pores reconstituted with β1-4 galactose-modified *O*-linked *N*-acetylglucosamine glycoproteins. *J. Biol. Chem.* 269:9289–9297.

Moore, M.S., and G. Blobel. 1993. The GTP-binding protein Ran/TC4 is required for protein import into the nucleus. *Nature (Lond.).* 365:661–663.

Moore, M.S., and G. Blobel. 1994. Purification of a Ran-interacting protein that is required for protein import into the nucleus. *Proc. Natl. Acad. Sci. USA.* 91:10212–10216.

Moroianu, J., G. Blobel, and A. Radu. 1995. Previously identified protein of uncertain function is karyopherin α and together with karyopherin β docks import substrate at nuclear pore complexes. *Proc. Natl. Acad. Sci. USA.* 92: 2008–2011.

Mutvei, A., S. Dihlmann, W. Herth, and E.C. Hurt. 1992. NSP1 depletion in yeast affects nuclear pore formation and nuclear accumulation. *Eur. J. Cell Biol.* 59:280–295.

Nehrbass, U., H. Kern, A. Mutvei, H. Horstmann, B. Marshallsay, and E.C. Hurt. 1990. NSP1: a yeast nuclear envelope protein localized at the nuclear pores exerts its essential function by its carboxy-terminal domain. *Cell.* 61: 979–989.

Nehrbass, U., E. Fabre, S. Dihlmann, W. Herth, and E.C. Hurt. 1993. Analysis of nucleo-cytoplasmic transport in a thermosensitive mutant of the nuclear pore protein NSP1. *Eur. J. Cell Biol.* 62:1–12.

Newport, J. 1987. Nuclear reconstitution in vitro: stages of assembly around protein-free DNA. *Cell.* 48:205–217.

Panté, N., and U. Aebi. 1994. Towards understanding the three-dimensional structure of the nuclear pore complex at the molecular level. *Curr. Opin. Struct. Biol.* 4:187–196.

Panté, N., R. Bastos, I. McMorrow, B. Burke, and U. Aebi. 1994. Interactions and three-dimensional localization of a group of nuclear pore complex proteins. *J. Cell Biol.* 126:603–617.

Paschal, B.M., and L. Gerace. 1995. Identification of NTF2, a cytosolic factor for nuclear import that interacts with nuclear pore complex protein p62. *J. Cell Biol.* 129:925–937.

Pemberton, L.F., M.P. Rout, and G. Blobel. 1995. Disruption of the nucleoporin gene *NUP133* results in clustering of nuclear pore complexes. *Proc. Natl. Acad. Sci. USA.* 92:1187–1191.

Powers, M.A., and D.J. Forbes. 1994. Cytosolic factors in nuclear transport: what's importin? *Cell.* 79:931–934.

Powers, M.A., C. Macaulay, F.R. Masiarz, and D.J. Forbes. 1995. Reconstituted nuclei depleted of a vertebrate GLFG nuclear pore protein, p97, import but are defective in nuclear growth and replication. *J. Cell Biol.* 128:721–736.

Radu, A., M.S. Moore, and G. Blobel. 1995. The peptide repeat domain of nucleoporin Nup98 functions as a docking site in transport across the nuclear pore complex. *Cell.* 81:215–222.

Rout, M.P., and G. Blobel. 1993. Isolation of the yeast nuclear pore complex. *J. Cell Biol.* 123:771–783.

Rout, M.P., and S.R. Wente. 1994. Pore for thought: nuclear pore complex proteins. *TIBS (Trends Biochem. Sci.).* 4:357–363.

Sanger, F., S. Nicklen, and A.R. Coulson. 1977. DNA-sequencing with chain-terminating inhibitors. *Proc. Natl. Acad. Sci. USA.* 74:5466–5467.

Schlaich, N.L., and E.C. Hurt. 1995. Analysis of nucleocytoplasmic transport and nuclear envelope structure in yeast disrupted for the gene encoding the nuclear pore protein Nup1p. *Eur. J. Cell Biol.* 67:8–14.

Schlenstedt, G., C. Saavedra, J.D.J. Loeb, C.N. Cole, and P.A. Silver. 1995. The GTP-bound form of the yeast Ran/TC4 homologue blocks nuclear protein import and appearance of poly $(A)^+$ RNA in the cytoplasm. *Proc. Natl. Acad. Sci. USA.* 92:225–229.

Sikorski, R.S., and R. Hieter. 1989. A system of shuttle vectors and yeast host strains designed for efficient manipulation of DNA in *Saccharomyces cerevisiae. Genetics.* 122:19–27.

Simos, G., and E.C. Hurt. 1995. Nucleocytoplasmic transport: factors and mechanisms. *FEBS Lett.* 369:107–112.

Simos, G., H. Tekotte, H. Grosjean, A. Segref, K. Sharma, D. Tollervey, and E.C. Hurt. 1996. Nuclear pore proteins are involved in the biogenesis of functional tRNA. *EMBO (Eur. Mol. Biol. Organ.) J.* 15:2270–2284.

Siniossoglou, S., C. Wimmer, M. Rieger, V. Doye, H. Tekotte, C. Weise, S. Emig, A. Segref, and E.C. Hurt. 1996. A novel complex of nucleoporins which includes Sec13p and a Sec13p homologue is essential for normal nuclear pores. *Cell.* 84:265–275.

Sukegawa, J., and G. Blobel. 1993. A nuclear pore complex protein that contains zinc finger motifs, binds DNA, and faces the nucleoplasm. *Cell.* 72:29–38.

Weis, K., I.W. Mattaj, and A.I. Lamond. 1995. Identification of hSRP1α as a functional receptor for nuclear localization sequences. *Science (Wash. DC).* 268:1049–1053.

Wente, S.R., and G. Blobel. 1993. A temperature-sensitive *NUP116* null mutant forms a nuclear envelope seal over the yeast nuclear pore complex thereby blocking nucleocytoplasmic traffic. *J. Cell Biol.* 123:275–284.

Wente, S.R., and G. Blobel. 1994. NUP145 encodes a novel yeast glycine-leucine-phenylalanine-glycine (GLFG) nucleoporin required for nuclear envelope structure. *J. Cell Biol.* 125:955–969.

Wilken, N., U. Kossner, J.-L. Senécal, U. Scheer, and M.-C. Dabauvalle. 1993. Nup180, a novel nuclear pore complex protein localizing to the cytoplasmic ring and associated fibrils. *J. Cell Biol.* 123:1345–1354.

Wimmer, C., V. Doye, P. Grandi, U. Nehrbass, and E. Hurt. 1992. A new subclass of nucleoporins that functionally interacts with nuclear pore protein NSP1. *EMBO (Eur. Mol. Biol. Organ.) J.* 11:5051–5061.

Wozniak, R.W., G. Blobel, and M.P. Rout. 1994. POM152 is an integral protein of the pore membrane domain of the yeast nuclear envelope. *J. Cell Biol.* 125:31–42.

Yokoyama, N., N. Hayashi, T. Seki, N. Panté, T. Ohba, K. Nishii, K. Kuma, T. Hayashida, T. Miyata, U. Aebi et al. 1995. A giant nucleopore protein that binds Ran/TC4. *Nature (Lond.).* 376:184–188.